

# Searches for new particles decaying into jet pairs in ATLAS data

*R M Buckingham for the ATLAS Collaboration*

*Department of Physics, University of Oxford, Denys Wilkinson Building, Keble Road,  
Oxford, OX1 3HR*

## 1 Introduction

Results are presented on the search for new physics in the dijet mass and angular distributions using data collected in 2010 and 2011 with the ATLAS detector at the LHC. Results of searches in dijet angular distributions with  $36 \text{ pb}^{-1}$  of data are taken from [1], whilst new results of searches in dijet mass distributions with  $163 \text{ pb}^{-1}$  of data collected in 2011 are shown for the first time [2].

No evidence for resonances was found in the updated sample. Improved limits are set on the product of cross section and acceptance for excited-quark ( $q^*$ ) and axigluon production as a function of  $q^*$  and axigluon mass. These exclude at the 95% CL the  $q^*$  mass interval  $0.80 < m_{q^*} < 2.49 \text{ TeV}$  and the axigluon mass interval  $0.80 < m < 2.67 \text{ TeV}$ . Production cross section limits as a function of dijet mass are also set using a simplified Gaussian signal model to facilitate comparisons with other hypotheses.

## 2 Searches for New Physics

Dijet signatures result from scattering processes well described within the Standard Model (SM) by perturbative quantum chromodynamics (QCD). However, it is possible for there to be additional contributions from new massive particles, or even new forces manifesting themselves at large center of mass (CM) energies.

Examples of new physics models include quark compositeness, excited quarks, TeV-scale gravity, micro-black holes and axigluons. (See [1] for further discussion.)

### 2.1 Dijet Angular Distributions

The angular variable  $\chi$  is determined from the rapidity<sup>1</sup>,  $y$ , of the two leading jets:  $\chi = \exp(2|y^*|)$ , where  $y^* = (y_1 - y_2)/2$ . The utility of the  $\chi$  variable arises because the  $\chi$

---

<sup>1</sup>The rapidity,  $y$  is defined as  $y = \frac{1}{2} \ln \left( \frac{1+|\cos \theta^*|}{1-|\cos \theta^*|} \right)$



distributions associated with final states produced via QCD interactions are relatively flat compared with the distributions associated with new particles or interactions that typically peak at low values of  $\chi$ . Plotting normalized  $\chi$  distributions in broad bins of dijet invariant mass allows identification of new threshold effects.

In order to also be sensitive to resonances, the new variable

$$F_\chi(m_{jj}) = \frac{N_{events}(|y^*| < 0.6)}{N_{events}(|y^*| < 1.7)} \quad (1)$$

is defined. This variable is sensitive to mass-dependent changes in the number of centrally produced dijet events.

Data is compared to LO PYTHIA Monte Carlo (MC), multiplied by bin-wise k-factors to account for next-to-leading order (NLO) contributions.

The resulting distributions are shown in Figure 1. Data is found to be consistent with QCD MC. For a full discussion of this analysis, including treatment of systematic uncertainties, calculation of  $p$ -values and limit-setting procedures, see [1].

Limits are set on new physical processes using  $\chi$  and  $F_\chi(m_{jj})$  with a frequentist  $CL_{s+b}$  approach. The resulting limits can be found in Table 1.

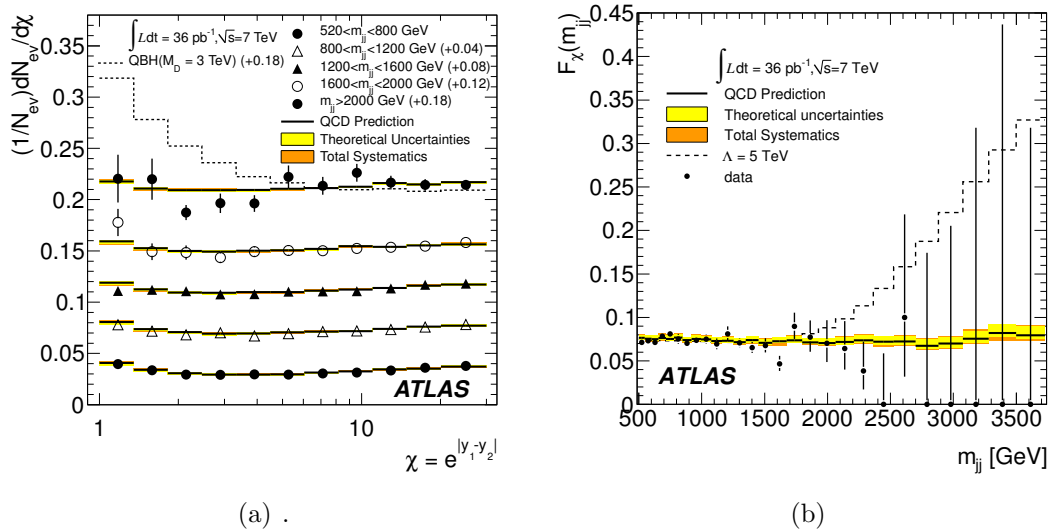


Figure 1: (a) The  $\chi$  distributions for  $520 < m_{jj} < 800$  GeV,  $800 < m_{jj} < 1200$  GeV,  $1200 < m_{jj} < 1600$  GeV,  $1600 < m_{jj} < 2000$  GeV and  $m_{jj} > 2000$  GeV and (b)  $F_\chi(m_{jj})$  distribution versus  $m_{jj}$ . Shown are the QCD predictions with systematic uncertainties (narrow bands), and data points with statistical uncertainties. Note that in (a) the distributions and QCD predictions have been offset by the amount shown in the legend to aid in visually comparing the shapes in each mass bin.

## 2.2 Dijet Resonance Searches

The dedicated dijet resonance search looks for bumps in the smooth and steeply falling dijet invariant mass spectrum:

$$m_{jj} = \sqrt{(E^{j_1} + E^{j_2})^2 - (\vec{p}^{j_1} + \vec{p}^{j_2})^2}, \quad (2)$$

In contrast to the angular analysis, the resonance analysis extracts the background hypothesis by fitting the data with the function: [3]

$$f(x) = p_1(1 - x)^{p_2} x^{p_3 + p_4 \ln x} \quad (3)$$

The resulting distribution is shown in Figure 2.

The BUMPHUNTER algorithm is used to locate the most discrepant region in the dijet spectrum (with respect to the background fit) and quantify its significance, whilst naturally incorporating the trials factor. The most significant bump is formed by the four bins from 3281 - 4230 GeV with a  $p$ -value of 0.25. Thus, there is no significant evidence for a resonance structure.

In the absence of new physics, a Bayesian method is used to set 95% credibility-level (CL) upper limits on  $\sigma \cdot \mathcal{A}$ . The result is shown in Figure 2. For a fuller description of the limit-setting procedure and treatment of systematic uncertainties, see [1].

In order to facilitate comparisons with other hypotheses, limits are also set on simplified Gaussian models. Gaussian distributions are considered for various means and widths. Limits are set at the 95% CL, including systematic uncertainties, on  $\sigma \cdot \mathcal{A}$ . The limits are presented in [2] (Table 3 and Figure 3).

A summary of the resulting limits from both angular and resonance analyses, for all considered models, is shown in Table 1.

## References

- [1] ATLAS Collaboration, *Search for New Physics in Dijet Mass and Angular Distributions in  $pp$  Collisions at  $\sqrt{s} = 7$  TeV Measured with the ATLAS Detector*, New Journal of Physics **13** (2011) 053044
- [2] ATLAS Collaboration, *Update of the Search for New Physics in Dijet Mass Distribution in  $163 \text{ pb}^{-1}$  of  $pp$  Collisions at  $\sqrt{s} = 7$  TeV Measured with the ATLAS Detector*, ATLAS-CONF-2011-081, <http://cdsweb.cern.ch/record/1355704>
- [3] CDF Collaboration, *Search for new particles decaying into dijets in proton-proton collisions at  $\sqrt{s} = 1.96$  TeV*, Phys. Rev. D **79** (2009) 112002

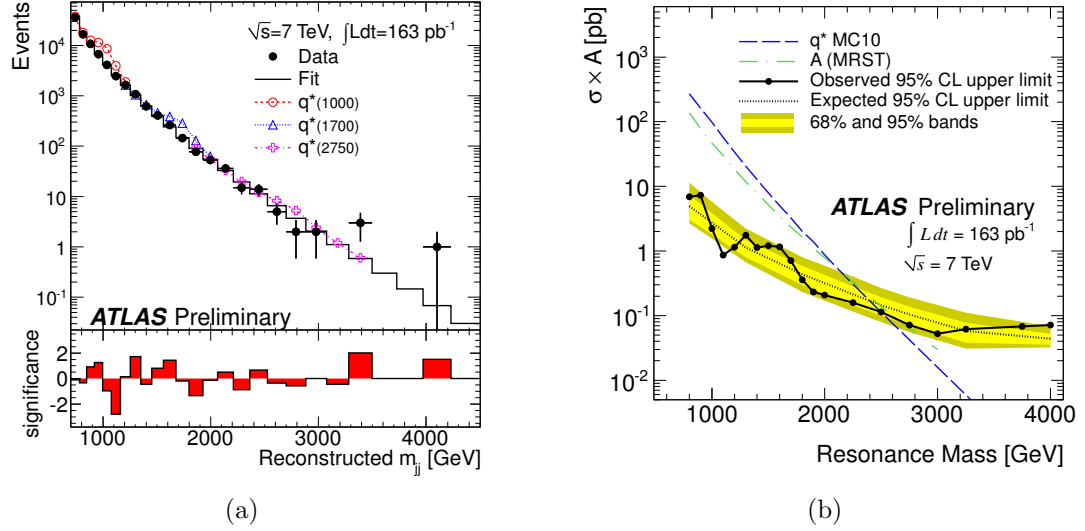


Figure 2: (a) Data dijet mass distribution (filled points) with background fit described by Eqn. 3 (histogram).  $q^*$  signals for excited-quark masses of 1, 1.7 and 2.75 TeV are plotted on top of the background.

(b) The 95% CL upper limit on  $\sigma \cdot \mathcal{A}$  as a function of dijet resonance mass (black filled circles). Black dotted curve shows the expected 95% CL upper limit and the light and dark yellow shaded bands represent the 68% and 95% contours, respectively.

Model and Analysis Strategy	95% C.L. Limits (TeV)	
	Expected	Observed
Excited Quark $q^*$		
Resonance in $m_{jj}$	2.40*	2.49*
$F_\chi(m_{jj})$	2.12	2.64
Quantum Black Holes for $n = 6$		
Resonance in $m_{jj}$	3.64	3.67
$F_\chi(m_{jj})$	3.49	3.78
Axigluon		
Resonance in $m_{jj}$	2.48*	2.67*
Contact Interaction $\Lambda$		
$F_\chi(m_{jj})$	5.7	9.5

Table 1: The 95% CL lower limits on the masses and energy scales of the models examined in [1, 2]. Limits marked with a \* correspond to limits with 163 pb<sup>-1</sup> of data [2], whilst the remainder are with 36 pb<sup>-1</sup> [1].